

The Thermodynamics of Quarks and Gluons*

Helmut Satz

Fakultät für Physik, Universität Bielefeld, Germany

Abstract:

This is an introduction to the study of strongly interacting matter. We survey its different possible states and discuss the transition from hadronic matter to a plasma of deconfined quarks and gluons. Following this, we summarize the results provided by lattice QCD finite temperature and density, and then investigate the nature of the deconfinement transition. Finally we give a schematic overview of possible ways to study the properties of the quark-gluon plasma.

arXiv:0803.1611v1 [hep-ph] 11 Mar 2008

* Lecture given at the *QGP Winter School*, Jaipur/India, Feb. 1, 2008; to appear in *Springer Lecture Notes in Physics*

1 Prelude

The fundamental questions of physics appear on two levels, the microscopic and macroscopic. We begin by asking:

- What are the ultimate constituents of matter?
- What are the basic forces between these constituents?

Given the basic building blocks and their interactions, we want to know:

- What are the possible states of matter?
- How do transitions between these states take place?

How far have we advanced today in our understanding of these different aspects?

According to our present state of knowledge, the ultimate constituents are quarks, leptons, gluons, photons, intermediate vector bosons (Z/W^\pm) and Higgs bosons - in a conservative count (no antiparticles etc.), sixteen in all, with gravitation not yet in the game.

Their interactions were originally classified as strong, electromagnetic, weak and gravitation, leaving a more general scheme as a challenge. The first unification brought electroweak theory, the second combined this with strong interactions to the standard model. The origin of all the different basic constituents, as well as the role of gravitation, are still open, waiting for the theory of everything (TOE).

In ancient times, the basic states of matter were earth, water, air and fire; today we have solids, liquids, gases and plasmas. In addition, there now is a multitude of others: insulators, conductors and superconductors, fluids and superfluids, ferromagnets, spin glasses, gelatines and many more. And the question of the possible states of matter brings us to a new kind of physics; the knowledge of the elementary constituents and their interactions in general does not predict the structure of the possible complex states of many constituents.

The study of complex systems becomes even more general, less dependent on the microstructure, when we ask for the transitions between the different states. We have phase transitions, depending on the singular behaviour of the partition function determined by the respective dynamics, as well as clustering and percolation transitions, determined by the connectivity aspects of the system. But we then find that scaling and renormalization concepts lead to a universal description of critical phenomena, and critical exponents define universality classes which contain quite different interaction forms.

When we study strongly interacting matter, we are therefore led to aspects which are relevant not only to QCD, but to the understanding of complex systems in general.

2 States of Strongly Interacting Matter

What happens to strongly interacting matter in the limit of high temperatures and densities? This question has fascinated physicists ever since the discovery of the strong force and the multiple hadron production it leads to. Let us look at some of the features that have emerged over the years.

- Hadrons have an intrinsic size, with a radius $r_h \simeq 1$ fm, and hence a hadron needs a space of volume $V_h \simeq (4\pi/3)r_h^3$ in order to exist. This suggests a limiting density n_c of hadronic matter [1], with $n_c = 1/V_h \simeq 1.5 n_0$, where $n_0 \simeq 0.17 \text{ fm}^{-3}$ denotes the density of normal nuclear matter.
- Hadronic interactions provide abundant resonance production, and the resulting number $\rho(m)$ of hadron species increases exponentially as function of the resonance mass m , $\rho(m) \sim \exp(b m)$. Such a form for $\rho(m)$ appeared first in the statistical bootstrap model, based on self-similar resonance formation or decay [2]. It was then also obtained in the more dynamical dual resonance approach [3]. In hadron thermodynamics, the exponential increase of the resonance degeneracy results in an upper limit for the temperature of hadronic matter, $T_c = 1/b \simeq 150 - 200$ MeV [2].
- What happens beyond T_c ? In QCD, hadrons are dimensionful color-neutral bound states of more basic pointlike colored quarks and gluons. Hadronic matter, consisting of colorless constituents of hadronic dimensions, can therefore turn at high temperatures and/or densities into a quark-gluon plasma of pointlike colored quarks and gluons as constituents [4]. This deconfinement transition leads to a colour-conducting state and thus is the QCD counterpart of the insulator-conductor transition in atomic matter [5].
- A shift in the effective constituent mass is a second transition phenomenon expected from the behavior of atomic matter. At $T = 0$, in vacuum, quarks dress themselves with gluons to form the constituent quarks that make up hadrons. As a result, the bare quark mass $m_q \sim 0$ is replaced by a constituent quark mass $M_q \sim 300$ MeV. In a hot medium, this dressing melts and $M_q \rightarrow 0$. Since the QCD Lagrangian for $m_q = 0$ is chirally symmetric, $M_q \neq 0$ implies spontaneous chiral symmetry breaking. The melting $M_q \rightarrow 0$ thus corresponds to chiral symmetry restoration. We shall see later on that in QCD, as in atomic physics, the shift of the constituent mass coincides with the onset of conductivity.
- A third type of transition would set in if the attractive interaction between quarks leads in the deconfined phase to the formation of colored bosonic diquark pairs, the Cooper pairs of QCD. These diquarks can then condense at low temperature to form a color superconductor. Heating will dissociate the diquark pairs and turn the color superconductor into a normal color conductor.

Using the baryochemical potential μ as a measure for the baryon density of the system, we thus expect the phase diagram of QCD to have the schematic form shown in Fig. 1. Given QCD as the fundamental theory of strong interactions, we can use the QCD Lagrangian as dynamics input to derive the resulting thermodynamics of strongly interacting matter. For vanishing baryochemical potential, $\mu = 0$, this can be evaluated with the help of the lattice regularisation, leading to finite temperature lattice QCD.

3 From Hadrons to Quarks and Gluons

Before turning to the results from lattice QCD, we illustrate the transition from hadronic matter to quark-gluon plasma by a very simple model. For an ideal gas of massless pions,

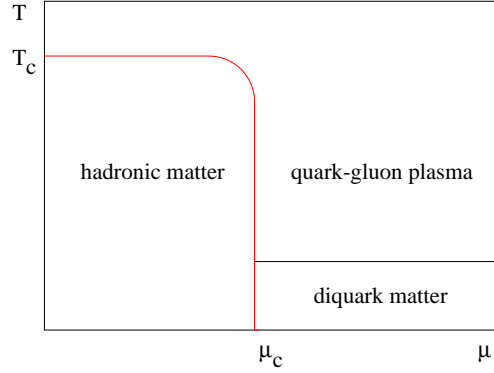


Figure 1: The phase diagram of QCD

the pressure as function of the temperature is given by the Stefan-Boltzmann form

$$P_\pi = 3 \frac{\pi^2}{90} T^4 \quad (1)$$

where the factor 3 accounts for the three charge states of the pion. The corresponding form for an ideal quark-gluon plasma with two flavours and three colours is

$$P_{gg} = \left\{ 2 \times 8 + \frac{7}{8} (3 \times 2 \times 2 \times 2) \right\} \frac{\pi^2}{90} T^4 - B = 37 \frac{\pi^2}{90} T^4 - B. \quad (2)$$

In Eq. (2), the first temperature term in the curly brackets accounts for the two spin and eight colour degrees of freedom of the gluons, the second for the three colour, two flavour, two spin and two particle-antiparticle degrees of freedom of the quarks, with $7/8$ to obtain the correct statistics. The bag pressure B takes into account the difference between the physical vacuum and the ground state for quarks and gluons in a medium.

Since in thermodynamics, a system chooses the state of lowest free energy and hence highest pressure, we compare in Fig. 2 a the temperature behaviour of Eq's. (1) and (2). Our simple model thus leads to a two-phase picture of strongly interacting matter, with a hadronic phase up to

$$T_c = \left(\frac{45}{17\pi^2} \right)^{1/4} B^{1/4} \simeq 0.72 B^{1/4} \quad (3)$$

and a quark gluon plasma above this critical temperature. From hadron spectroscopy, the bag pressure is given by $B^{1/4} \simeq 0.2 \text{ GeV}$, so that we obtain

$$T_c \simeq 150 \text{ MeV} \quad (4)$$

as the deconfinement temperature. In the next section we shall find this simple estimate to be remarkably close to the value obtained in lattice QCD.

The energy densities of the two phases of our model are given by

$$\epsilon_\pi = \frac{\pi^2}{10} T^4 \quad (5)$$

and

$$\epsilon_{gg} = 37 \frac{\pi^2}{30} T^4 + B. \quad (6)$$

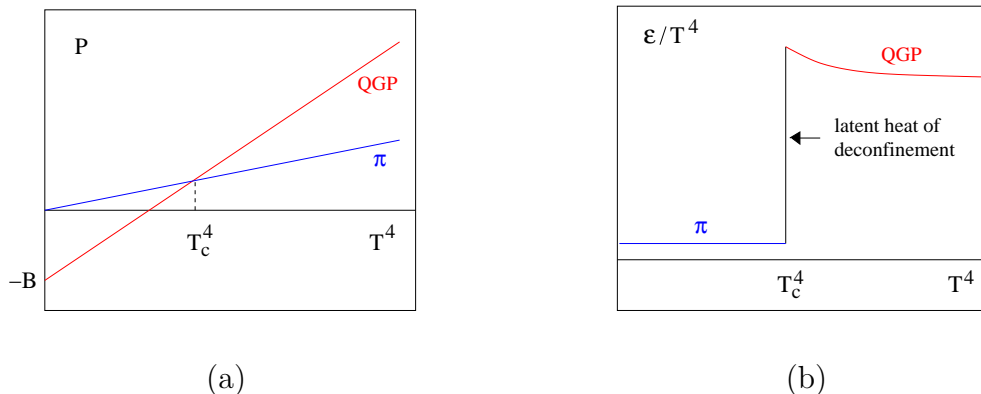


Figure 2: Pressure and energy density in a two-phase ideal gas model.

By construction, the transition is first order, and the resulting temperature dependence is shown in Fig. 2 b. At T_c , the energy density increases abruptly by the latent heat of deconfinement. We note that even though both phases consist of massless non-interacting constituents, the dimensionless “interaction measure”

$$\frac{\epsilon - 3P}{T^4} = \frac{4B}{T^4} \quad (7)$$

does not vanish in the quark-gluon plasma, due to the (non-perturbative) difference between physical vacuum and in-medium QCD ground state [6].

4 Finite Temperature Lattice QCD

We now want to show that the conceptual considerations of the last section indeed follow from strong interaction thermodynamics as based on QCD as the input dynamics. QCD is defined by the Lagrangian

$$\mathcal{L} = -\frac{1}{4}F_{\mu\nu}^a F_a^{\mu\nu} - \sum_f \bar{\psi}_\alpha^f (i\gamma^\mu \partial_\mu + m_f - g\gamma^\mu A_\mu)^{\alpha\beta} \psi_\beta^f, \quad (8)$$

with

$$F_{\mu\nu}^a = (\partial_\mu A_\nu^a - \partial_\nu A_\mu^a - gf_{bc}^a A_\mu^b A_\nu^c). \quad (9)$$

Here A_μ^a denotes the gluon field of colour a ($a=1,2,\dots,8$) and ψ_α^f the quark field of colour α ($\alpha=1,2,3$) and flavour f ; the input (‘bare’) quark masses are given by m_f . With the dynamics thus determined, the corresponding thermodynamics is obtained from the partition function, which is most suitably expressed as a functional path integral,

$$Z(T, V) = \int dA d\psi d\bar{\psi} \exp \left(- \int_V d^3x \int_0^{1/T} d\tau \mathcal{L}(A, \psi, \bar{\psi}) \right), \quad (10)$$

since this form involves directly the Lagrangian density defining the theory. The spatial integration in the exponent of Eq. (10) is performed over the entire spatial volume V of the system; in the thermodynamic limit it becomes infinite. The time component x_0 is “rotated” to become purely imaginary, $\tau = ix_0$, thus turning the Minkowski manifold, on

which the fields A and ψ are originally defined, into a Euclidean space. The integration over τ in Eq. (10) runs over a finite slice whose thickness is determined by the temperature of the system.

From $Z(T, V)$, all thermodynamical observables can be calculated in the usual fashion. Thus

$$\epsilon = (T^2/V) \left(\frac{\partial \ln Z}{\partial T} \right)_V \quad (11)$$

gives the energy density, and

$$P = T \left(\frac{\partial \ln Z}{\partial V} \right)_T \quad (12)$$

the pressure. For the study of critical behaviour, long range correlations and multi-particle interactions are of crucial importance; hence perturbation theory cannot be used. The necessary non-perturbative regularisation scheme is provided by the lattice formulation of QCD [7]; it leads to a form which can be evaluated numerically by computer simulation [8].

The calculational methods and techniques of finite temperature lattice QCD form a challenging subject on its own, which certainly surpasses the scope of this survey. We therefore restrict ourselves here to a summary of the main results obtained so far; for more details, we refer to excellent recent surveys and reviews [9].

The first variable considered in finite temperature lattice QCD is the deconfinement measure provided by the Polyakov loop [10, 11]

$$L(T) \sim \lim_{r \rightarrow \infty} \exp\{-V(r)/T\} \quad (13)$$

where $V(r)$ is the potential between a static quark-antiquark pair separated by a distance r . In pure gauge theory, without light quarks, $V(r) \sim \sigma r$, where σ is the string tension; hence here $V(\infty) = \infty$, so that $L = 0$. In a deconfined medium, colour screening among the gluons leads to a melting of the string, which makes $V(r)$ finite at large r ; hence now L does not vanish. It thus becomes an ‘order parameter’ like the magnetisation in the Ising model: for the temperature range $0 \leq T \leq T_c$, we have $L = 0$ and hence confinement, while for $T_c < T$ we have $L > 0$ and deconfinement. The temperature T_c at which L becomes finite thus defines the onset of deconfinement.

In the large quark mass limit, QCD reduces to pure $SU(3)$ gauge theory, which is invariant under a global Z_3 symmetry. The Polyakov loop provides a measure of the state of the system under this symmetry: it vanishes for Z_3 symmetric states and becomes finite when Z_3 is spontaneously broken. Hence the critical behaviour of $SU(3)$ gauge theory is in the same universality class as that of Z_3 spin theory (the 3-state Potts model): both are due to the spontaneous symmetry breaking of a global Z_3 symmetry [12].

For finite quark mass m_q , $V(r)$ remains finite for $r \rightarrow \infty$, since the ‘string’ between the two colour charges ‘breaks’ when the corresponding potential energy becomes equal to the mass M_h of the lowest hadron; beyond this point, it becomes energetically more favourable to produce an additional hadron. Hence now L no longer vanishes in the confined phase, but only becomes exponentially small there,

$$L(T) \sim \exp\{-M_h/T\}; \quad (14)$$

here M_h is of the order of the ρ -mass, so that $L \sim 10^{-2}$, rather than zero. Deconfinement is thus indeed much like the insulator-conductor transition, for which the order parameter, the conductivity $\sigma(T)$, also does not really vanish for $T > 0$, but with $\sigma(T) \sim \exp\{-\Delta E/T\}$ is only exponentially small, since thermal ionisation (with ionisation energy ΔE) produces a small number of unbound electrons even in the insulator phase.

Fig. 3a shows recent lattice results for $L(T)$ and the corresponding susceptibility $\chi_L(T) \sim \langle L^2 \rangle - \langle L \rangle^2$ [13]. The calculations were performed for the case of two flavours of light quarks, using a current quark mass about four times larger than that needed for the physical pion mass. We note that $L(T)$ undergoes the expected sudden increase from a small confinement to a much larger deconfinement value. The sharp peak of $\chi_L(T)$ defines quite well the transition temperature T_c , which we shall shortly specify in physical units.

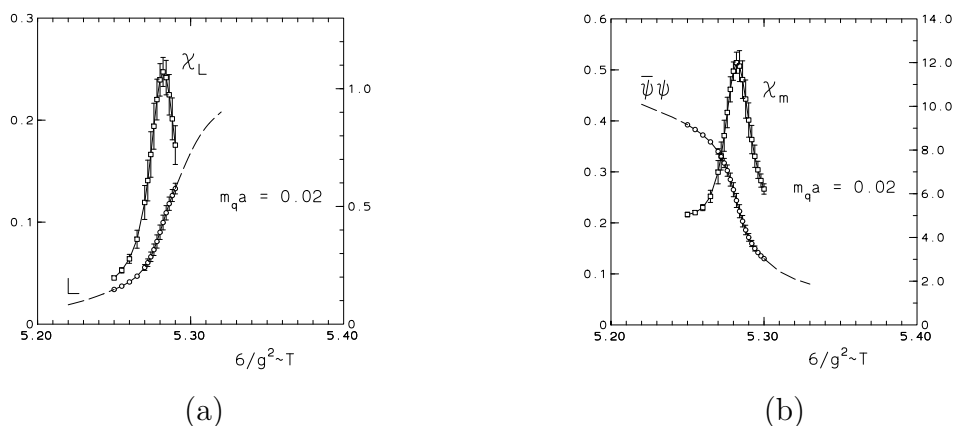


Figure 3: Polyakov loop and chiral condensate in two-flavour QCD [13]

The next quantity to consider is the effective quark mass; it is measured by the expectation value of the corresponding term in the Lagrangian, $\langle \bar{\psi}\psi \rangle(T)$. In the limit of vanishing current quark mass, the Lagrangian becomes chirally symmetric and $\langle \bar{\psi}\psi \rangle(T)$ the corresponding order parameter. In the confined phase, with effective constituent quark masses $M_q \simeq 0.3$ GeV, this chiral symmetry is spontaneously broken, while in the deconfined phase, at high enough temperature, we expect its restoration. In the real world, with finite pion and hence finite current quark mass, this symmetry is also only approximate, since $\langle \bar{\psi}\psi \rangle(T)$ now never vanishes at finite T .

The behaviour of $\langle \bar{\psi}\psi \rangle(T)$ and the corresponding susceptibility $\chi_m \sim \partial \langle \bar{\psi}\psi \rangle / \partial m_q$ are shown in Fig. 3 b [13], calculated for the same case as above in Fig. 3 a. We note here the expected sudden drop of the effective quark mass and the associated sharp peak in the susceptibility. The temperature at which this occurs coincides with that obtained through the deconfinement measure. We therefore conclude that at vanishing baryon number density, quark deconfinement and the shift from constituent to current quark mass coincide.

We thus obtain for $\mu_B = 0$ a rather well defined phase structure, consisting of a confined phase for $T < T_c$, with $L(T) \simeq 0$ and $\langle \bar{\psi}\psi \rangle(T) \neq 0$, and a deconfined phase for $T > T_c$ with $L(T) \neq 0$ and $\langle \bar{\psi}\psi \rangle(T) \simeq 0$. The underlying symmetries associated to the critical

behaviour at $T = T_c$, the Z_3 symmetry of deconfinement and the chiral symmetry of the quark mass shift, become exact in the limits $m_q \rightarrow \infty$ and $m_q \rightarrow 0$, respectively. In the real world, both symmetries are only approximate; nevertheless, we see from Fig. 3 that both associated measures retain an almost critical behaviour.

Next we come to the behaviour of energy density ϵ and pressure P at deconfinement [14]. In Fig. 4, it is seen that ϵ/T^4 changes quite abruptly at the above critical temperature T_c , increasing from a low hadronic value to one slightly below that expected for an ideal gas of massless quarks and gluons [15].

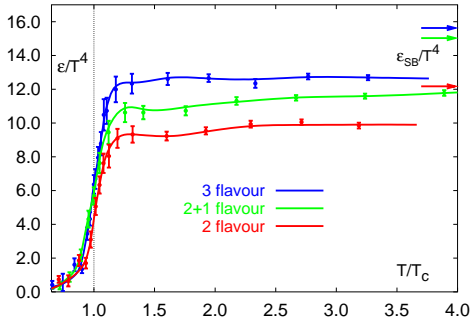


Figure 4: Energy density vs. temperature [15]

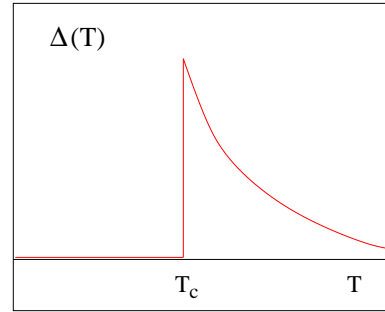


Figure 5: Interaction measure vs. temperature [15]

Besides the sudden increase at deconfinement, there are two further points to note. In the region $T_c < T < 2 T_c$, there still remain strong interaction effects. As seen in Fig. 5, the ‘interaction measure’ $\Delta = (\epsilon - 3P)/T^4$ remains sizeable and does not vanish, as it would for an ideal gas of massless constituents. In the simple model of the previous section, such an effect arose due to the bag pressure, and in actual QCD, one can also interpret it in such a fashion [6]. It has also been considered in terms of a gradual onset of deconfinement starting from high momenta [16], and most recently as a possible consequence of coloured “resonance” states [17]. The second point to note is that the thermodynamic observables remain about 10 % below their Stefan-Boltzmann values (marked “SB” in Fig. 4) even at very high temperatures, where the interaction measure becomes very small. Such deviations from ideal gas behaviour can be expressed to a large extent in terms of effective ‘thermal’ masses m_{th} of quarks and gluons, with $m_{\text{th}} \simeq g(T) T$ [18] - [20]. Maintaining the next-to-leading order term in mass in the Stefan-Boltzmann form gives for the pressure

$$P = c T^4 \left[1 - a \left(\frac{m_{\text{th}}}{T} \right)^2 \right] = c T^4 [1 - a g^2(T)] \quad (15)$$

and for the energy density

$$\epsilon = 3 c T^4 \left[1 - \frac{a}{3} \left(\frac{m_{\text{th}}}{T} \right)^2 - \frac{2a}{3} \left(\frac{m_{\text{th}}}{T} \right) \left(\frac{dm_{\text{th}}}{dT} \right) \right] = 3 c T^4 \left[1 - a g^2(T) - \frac{2a m_{\text{th}}}{3} \left(\frac{dg}{dT} \right) \right], \quad (16)$$

where c and a are colour- and flavour-dependent positive constants. Since $g(T) \sim 1/\log T$, the deviations of P and ϵ from the massless Stefan-Boltzmann form vanish as $(\log T)^{-2}$, while the interaction measure

$$\Delta \sim \frac{1}{(\log T)^3} \quad (17)$$

decreases more rapidly by one power of $\log T$.

Finally we turn to the value of the transition temperature. Since QCD (in the limit of massless quarks) does not contain any dimensional parameters, T_c can only be obtained in physical units by expressing it in terms of some other known observable which can also be calculated on the lattice, such as the ρ -mass, the proton mass, or the string tension. In the continuum limit, all different ways should lead to the same result. Within the present accuracy, they define the uncertainty so far still inherent in the lattice evaluation of QCD. Using the ρ -mass to fix the scale leads to $T_c \simeq 0.15$ GeV, while the string tension still allows values as large as $T_c \simeq 0.20$ GeV. Very recently, fine structure charmonium calculations (the mass splitting between J/ψ , χ_c and ψ') have been used to fix the dimensional scale, leading to [21] to $T_c \simeq 190 \pm 10$ MeV. In any case, energy densities of some 1 - 2 GeV/fm³ are needed in order to produce a medium of deconfined quarks and gluons.

In summary, finite temperature lattice QCD at vanishing baryon density shows

- that there is a transition leading to colour deconfinement coincident with chiral symmetry restoration at $T_c \simeq 0.15 - 0.20$ GeV;
- that this transition is accompanied by a sudden increase in the energy density (the “latent heat of deconfinement”) from a small hadronic value to a much larger value, about 10 % below that of an ideal quark-gluon plasma.

In the following section, we want to address in more detail the nature of the critical behaviour encountered at the transition.

5 The Nature of the Transition

We begin with the behaviour for vanishing baryon density ($\mu = 0$) and come to $\mu \neq 0$ at the end. Consider the case of three quark species, u , d , s .

- In the limit $m_q \rightarrow \infty$ for all quark species, we recover pure $SU(3)$ gauge theory, with a deconfinement phase transition provided by spontaneous Z_3 breaking. It is first order, as is the case for the corresponding spin system, the 3-state Potts model.
- For $m_q \rightarrow 0$ for all quark masses, the Lagrangian becomes chirally symmetric, so that we have a phase transition corresponding to chiral symmetry restoration. In the case of three massless quarks, the transition is also of first order.
- For $0 < m_q < \infty$, there is neither spontaneous Z_3 breaking nor chiral symmetry restoration. Hence in general, there is no singular behaviour, apart from the transient disappearance of the first order discontinuities on a line of second order transitions. Beyond this, there is no genuine phase transition, but only a “rapid cross-over” from confinement to deconfinement. The overall behaviour is summarized in Fig. 6.
- As already implicitly noted above, both “order parameters” $L(T)$ and $\chi(T)$ nevertheless show a sharp temperature variation for all values of m_q , so that it is in fact possible to define quite well a common cross-over point T_c .

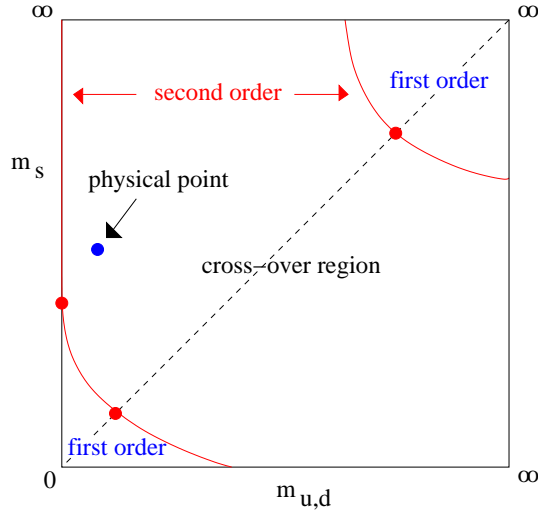


Figure 6: The nature of thermal critical behaviour in QCD

- The nature of the transition thus depends quite sensitively on the number of flavours N_f and the quark mass values: it can be a genuine phase transition (first order or continuous), or just a rapid cross-over. The case realized in nature, the “physical point”, corresponds to small u , d masses and a larger s -quark mass. It is fairly certain today that this point falls into the cross-over region.
- Finally we consider briefly the case of finite baryon density, $\mu \neq 0.$, so that the number of baryons exceeds that of antibaryons. Here the conventional computer algorithms of lattice QCD break down, and hence new calculation methods have to be developed. First such attempts (reweighting [22], analytic continuation [24], power series [25]) suggest for two light quark flavours the phase diagram shown in Fig. 7. It shows non-singular in a region between $0 \leq \mu < \mu_t$, a tricritical point at μ_t , and beyond this a first order transition. Recent lattice calculations provide some support for such behaviour; as shown in Fig. 8, the baryon density fluctuations appear to diverge for some critical value of the baryochemical potential [25].

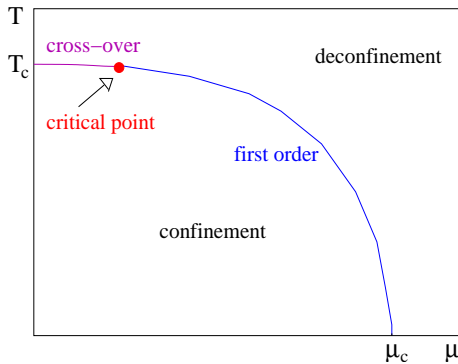


Figure 7: Phase structure in terms of the baryon density

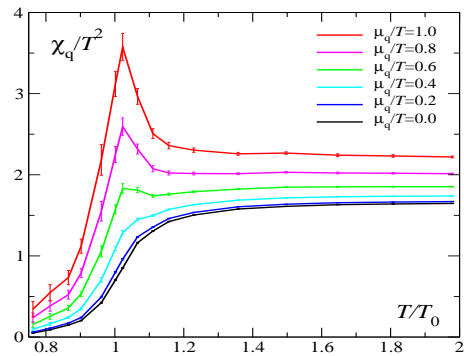


Figure 8: Baryon number susceptibility χ_q vs. temperature

The critical behaviour for strongly interacting matter at low or vanishing baryon density, describing the onset of confinement in the early universe and in high energy nuclear collisions, thus occurs in the rather enigmatic form of a “rapid cross-over”. There is no thermal singularity and hence, in a strict sense, there are neither distinct states of matter nor phase transitions between them. So what does the often mentioned experimental search for a “new state of matter” really mean? How can a new state appear without a phase transition? Is there a more general way to define and distinguish different states of bulk media? After all, in statistical QCD one does find that thermodynamic observables – energy and entropy densities, pressure, as well as the “order parameters” $L(T)$ and $\chi(T)$ – continue to change rapidly and thus define a rather clear transition line in the entire cross-over region. Why is this so, what is the mechanism which causes such a transition?

In closing this section, we consider a speculative answer to this rather fundamental question [26]. The traditional phase transitions, such as the freezing of water or the magnetization of iron, are due to symmetry breaking and the resulting singularities of the partition function. But there are other “transitions”, such as making pudding or boiling an egg, where one also has two clearly different states, but no singularities in the partition function. Such “liquid-gel” transitions are generally treated in terms of cluster formation and percolation [27]. They also correspond to critical behaviour, but the quantities that diverge are geometric (cluster size) and cannot be obtained from the partition function.

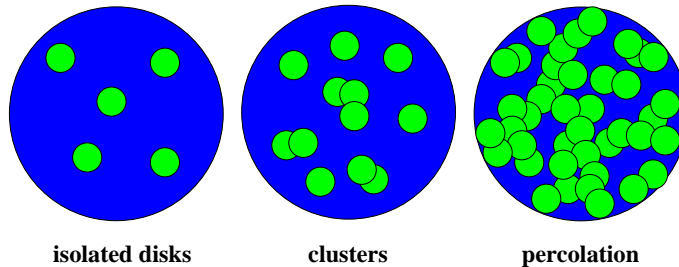


Figure 9: Lilies on a pond

The simplest example of this phenomenon is provided by two-dimensional disk percolation, something poetically called “lilies on a pond” (see Fig. 9). More formally: one distributes small disks of area $a = \pi r^2$ randomly on a large surface $A = \pi R^2$, $R \gg r$, with overlap allowed. With an increasing number of disks, clusters begin to form. If the large surface were water and the small disks floating water lilies: how many lilies are needed for a cluster to connect the opposite sides, so that an ant could walk across the pond without getting its feet wet? Given N disks, the disk density is $n = N/A$. Clearly, the average cluster $S(n)$ size will increase with n . The striking feature is that it does so in a very sudden way (see Fig. 10); as n approaches some “critical value” n_c , $S(n)$ suddenly becomes large enough to span the pond. In fact, in the limit $N \rightarrow \infty$ and $A \rightarrow \infty$ at constant n , both $S(n)$ and $dS(n)/dn$ diverge for $n \rightarrow n_c$: we have percolation as a geometric form of critical behaviour.

The critical density for the onset of percolation has been determined (numerically) for a variety of different systems. In two dimensions, disks percolate at $n_c \simeq 1.13/(\pi r^2)$, i.e., when we have a little more than one disk per unit area. Because of overlap, at this point

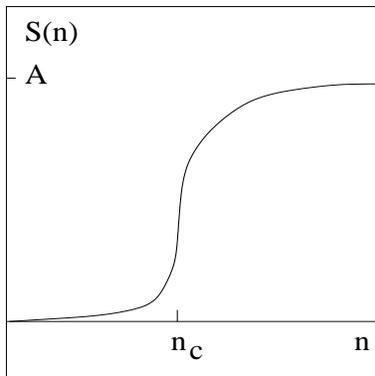


Figure 10: Cluster size $S(n)$ vs. density n

only 68% of space is covered by disks, 32% remain empty. Nevertheless, when our ant can walk across, a ship can no longer cross the pond, and vice versa. This is a special feature of two dimensions (the “fence effect”), and no longer holds for $d > 2$.

In three dimensions, the corresponding problem is one of overlapping spheres in a large volume. Here the critical density for the percolating spheres becomes $n_c \simeq 0.34/[(4\pi/3)r^3]$, with r denoting the radius of the little spheres now taking the place of the small disks we had in two dimensions. At the critical point in three dimensions, however, only 29% of space is covered by overlapping spheres, while 71% remains empty, and here both spheres and empty space form infinite connected networks. If we continue to increase the density of spheres, we reach a second critical point at $\bar{n}_c \simeq 1.24/[(4\pi/3)r^3]$, at which the vacuum stops to form an infinite network: now 71% of space is covered by spheres, and for $n > \bar{n}_c$, only isolated vacuum bubbles remain.

Let us then consider hadrons of intrinsic size $V_h = (4\pi/3)r_h^3$, with $r_h \simeq 0.8$ fm. In three-dimensional space, the formation of a connected large-scale cluster first occurs at the density

$$n_c = \frac{0.34}{V_h} \simeq 0.16 \text{ fm}^{-3}. \quad (18)$$

This point specifies the onset of hadronic *matter*, in contrast to a gas of hadrons, and it indeed correctly reproduces the density of normal nuclear matter. However, at this density the vacuum as connected medium also still exists (see Fig. 11a).

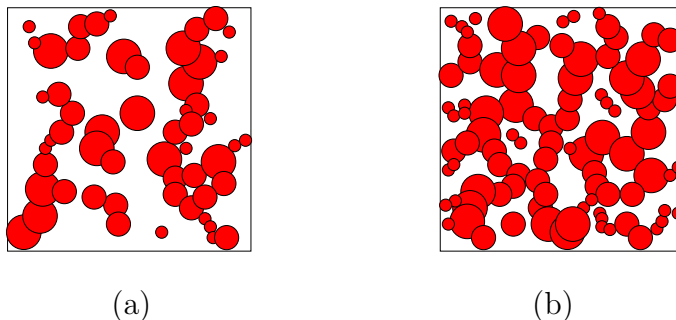


Figure 11: Hadron and vacuum percolation thresholds

To prevent infinite connecting vacuum clusters, a much higher hadron density is needed, as we saw above. Measured in hadronic size units, the vacuum disappears for

$$\bar{n}_c = \frac{1.24}{V_h} \simeq 0.56 \text{ fm}^{-3}, \quad (19)$$

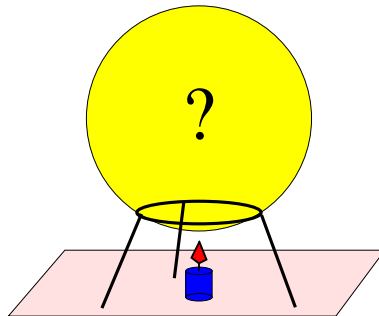
schematically illustrated in Fig. 11b. If we assume that at this point, the medium is of an ideal gas of all known hadrons and hadronic resonances, then we can calculate the temperature of the gas at the density \bar{n}_c : $n_{\text{res}}(T_c) = \bar{n}_c$ implies $T_c \simeq 170$ MeV, which agrees quite well with the value of the deconfinement temperature found in lattice QCD for $\mu = 0$.

We can thus use percolation to define the states of hadronic matter. At low density, we have a hadron gas, which at the percolation point n_c turns into connected hadronic matter. When this becomes so dense that only isolated vacuum bubbles survive, at \bar{n}_c , it turns into a quark-gluon plasma. This approach provides the correct values both for the density of standard nuclear matter and for the deconfinement transition temperature.

Such considerations may in fact well be of a more general nature than the problem of states and transitions in strong interaction physics. The question of whether symmetry or connectivity (cluster formation) determines the different states of many-body systems has intrigued theorists in statistical physics for a long time [28]. The lesson learned from spin systems appears to be that cluster formation and the associated critical behaviour are the more general features, which under certain conditions can also lead to thermal criticality, i.e., singular behaviour of the partition function.

6 Probing the Quark-Gluon Plasma

We thus find that at sufficiently high temperatures and/or densities, strongly interacting matter will be in a new state, consisting of deconfined quarks and gluons. How can we probe the properties of this state, how can we study its features as function of temperature and density? We want to address this question here in the sense of Einstein, who told us to make things as simple as possible, but not simpler. So let us start with a theorist's experimental set-up, consisting of a volume of unknown strongly interacting matter and a Bunsen burner, to heat it up and thus increase its energy density.



There are a number of methods we can use to study the unknown matter in our container:

- hadron radiation,
- electromagnetic radiation,
- dissociation of a passing quarkonium beam,
- energy loss of a passing hard jet.

All methods will be dealt with in detail during the course of this school. Here we just want to have a brief first look.

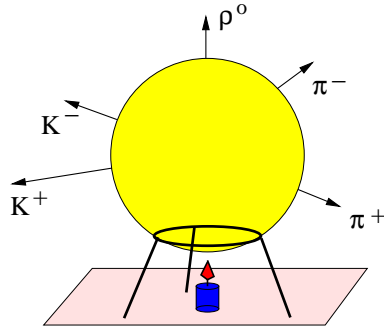


Figure 12: Hadron radiation

First of all, we note that the unknown medium radiates, since its temperature is (by assumption) much higher than that of its environment. Hadron radiation means that we study the emission of hadrons consisting of light (u, d, s) quarks; their size is given by the typical hadronic scale of about $1 \text{ fm} \simeq 1/(200 \text{ MeV})$. Since they cannot exist inside a deconfined medium, they are formed at the transition surface between the QGP and the physical vacuum. The physics of this surface is independent of the interior - the transition from deconfinement to confinement occurs at a temperature $T \simeq 160 - 180 \text{ MeV}$, no matter how hot the QGP initially was or still is in the interior of our volume. This is similar to having hot water vapor inside a glass container kept in a cool outside environment: at the surface, the vapor will condense into liquid, at a temperature of 100°C - no matter how hot it is in the middle. As a result, studying soft hadron production in high energy collisions will provide us with information about the hadronization transition, but not about the hot QGP. The striking observation that the relative hadron abundances in all high energy collisions are the same, from e^+e^- annihilation to hadron-hadron and heavy ion interactions, and that they correspond to those of an ideal resonance gas at $T \simeq 170 \text{ MeV}$, is a direct consequence of this fact [2, 29] .

Hadron radiation, as we have pictured it here, is oversimplified from the point of view of heavy ion interactions. In the case of static thermal radiation, at the point of hadronization all information about the earlier stages of the medium is lost, as we had noted above. If, however, the early medium has a very high energy density and can expand freely, i.e., is not constrained by the walls of a container, then this expansion will lead to a global hydrodynamic flow [30], giving an additional overall boost in momentum to the produced

hadrons: they will experience a “radial flow” depending on the initial energy density (see Fig. 13). Moreover, if the initial conditions were not spherically symmetric, as is in fact the cases in peripheral heavy ion collisions, the difference in pressure in different spatial directions will lead to a further “directed” or “elliptic” flow. Since both forms of flow thus do depend on the initial conditions, flow studies of hadron spectra can, at least in principle, provide information about the earlier, pre-hadronic stages.

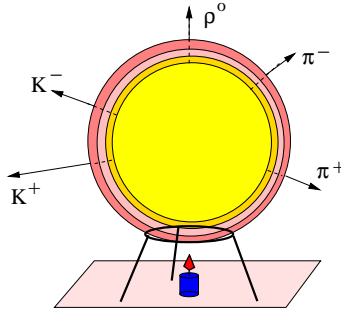


Figure 13: Radial flow and hadron radiation

The unknown hot medium also radiates electromagnetically, i.e., it emits photons and dileptons (e^+e^- or $\mu^+\mu^-$ pairs) [31]. These are formed either by the interaction of quarks and/or gluons, or by quark-antiquark annihilation. Since the photons and leptons interact only electromagnetically, they will, once they are formed, leave the medium without any further modification. Hence their spectra provide information about the state of the medium at the place or the time they were formed, and this can be in its deep interior or at very early stages of its evolution. Photons and dileptons thus do provide a possible probe of the hot QGP. The only problem is that they can be formed anywhere and at any time, even at the cool surface or by the emitted hadrons. The task in making them a viable tool is therefore the identification of the hot “thermal” radiation indeed emitted by the QGP.

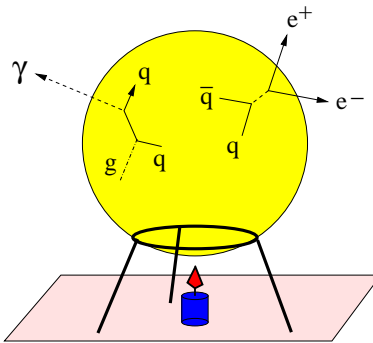


Figure 14: Electromagnetic radiation

Both electromagnetic and hadronic radiation are emitted by the medium itself, and they provide some information about the state of the medium at the time of emission. Another possible approach is to test the medium with an outside probe, and here we have two so far quite successful examples, quarkonia and jets.

Quarkonia are a special kind of hadrons, bound states of a heavy (c or b) quark and its antiquark. For the ground states J/ψ and Υ the binding energies are around 0.6 and 1.2 GeV, respectively, and thus much larger than the typical hadronic scale $\Lambda \sim 0.2$ GeV; as a consequence, they are also much smaller, with radii of about 0.1 and 0.2 fm. It is therefore expected that they can survive in a quark-gluon plasma through some range of temperatures above T_c , and this is in fact confirmed by lattice studies [32].

The higher excited quarkonium states are less tightly bound and hence larger, although their binding energies are in general still larger, their radii still smaller, than those of the usual light quark hadrons. Take the charmonium spectrum as example: the radius of the $J/\psi(1S)$ is about 0.2 fm, that of the $\chi_c(1P)$ about 0.3 fm, and that of the $\psi'(2S)$ 0.4 fm. Since deconfinement is related to colour screening, the crucial quantity for dissociation of a bound state is the relation of binding to screening radius. We therefore expect that the different charmonium states have different “melting temperatures” in a quark-gluon plasma. Hence the spectral analysis of in-medium quarkonium dissociation should provide a QGP thermometer [33].

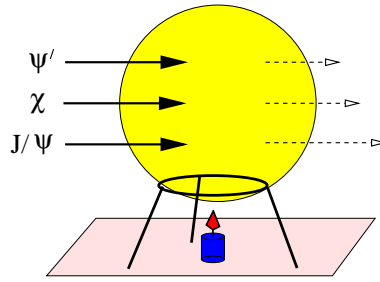


Figure 15: Charmonium suppression

As probe, we then shoot beams of specific charmonia (J/ψ , χ_c , ψ') into our medium sample and check which comes out on the other side (Fig. 15). If all three survive, we have an upper limit on the temperature, and by checking at just what temperature the ψ' , the χ_c and the J/ψ are dissociated, we have a way of specifying the temperature of the medium [34], as illustrated in Fi. 16.

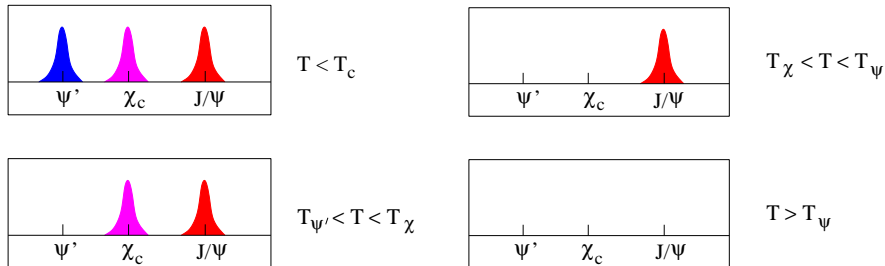


Figure 16: Charmonia as thermometer

Another possible probe is to shoot an energetic parton, quark or gluon, into our medium to be tested. How much energy it loses when it comes out on the other side will tell us

something about the density of the medium [35]. In particular, the density increases by an order of magnitude or more in the course of the deconfinement transition, and so the energy loss of a fast passing colour charge is expected to increase correspondingly (Fig. 17). Moreover, for quarks, the amount of jet quenching is predicted to depend on the mass of the quarks.

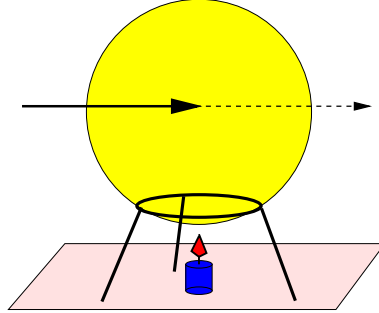


Figure 17: Jet quenching

In using quarkonia and jets as tools, we have so far considered a simplified situation, in which we test a given medium with distinct external probes. In heavy ion collisions, we have to create the probe in the same collision in which we create the medium. Quarkonia and jets (as well as open charm/beauty and very energetic dileptons and photons) constitute so-called “hard probes”, whose production occurs at the very early stages of the collision, before the medium is formed; they are therefore indeed present when it appears. Moreover, their production involves large energy/momentum scales and can be calculated by perturbative QCD techniques and tested in pp/pA collisions, so that behaviour and strength of such outside “beams” or “colour charges” are indeed quite well known.

7 Summary

We have shown that strong interaction thermodynamics leads to a well-defined transition from hadronic matter to a plasma of deconfined quarks and gluons. For vanishing baryon number density, the transition leads to simultaneous deconfinement and chiral symmetry restoration at $T_c \simeq 160 - 190$ MeV. At this point, the energy density increases by an order of magnitude through the latent heat of deconfinement.

The properties of the new medium above T_c , the quark-gluon plasma, can be studied through hard probes (quarkonium and open charm/beauty production, jet quenching) and electromagnetic radiation (photons and dileptons). Information about transition aspects is provided by light hadron radiation; through hydrodynamic flow, this can also shed light on pre-hadronic features.

References

- [1] I. Ya. Pomeranchuk, Doklady Akad. Nauk. SSSR 78
- [2] R. Hagedorn, Nuovo Cim. Suppl. 3 (1965) 147;
Nuovo Cim. 56A (1968) 1027.
- [3] K. Bardakci and S. Mandelstam, Phys. Rev. 184 (1969) 1640;
S. Fubini and G. Veneziano, Nuovo Cim. 64A (1969) 811.
- [4] N. Cabibbo and G. Parisi, Phys. Lett. 59 B (1975) 67.
- [5] H. Satz, Fortsch. Physik 33 (1985) 259.
- [6] M. Asakawa and T. Hatsuda, Nucl. Phys. A 610 (1996) 470c.
- [7] K. Wilson, Phys. Rev. D10 (1974) 2445.
- [8] M. Creutz, Phys. Rev. D 21 (1980) 2308.
- [9] For textbooks, surveys and further literature, see
I. Montvay and G. Münster, *Quantum Fields on a Lattice*, Cambridge University Press 1994;
H. J. Rothe, *Lattice Gauge Theory*, World Scientific Lecture Notes in Physics 59 (1997);
F. Karsch, Lect. Notes Phys. (Springer) 583 (2002) 209;
F. Karsch and E. Laermann, in *Quark-Gluon Plasma 3*, R. C. Hwa and X.-N. Wang (Eds.), World Scientific, Singapore 2004;
F. Karsch, arXiv[hep-lat] 0711.0661 and 0711.0656.
- [10] L. D. McLerran and B. Svetitsky, Phys. Lett. 98 B (1981) 195 and Phys. Rev. D 24 (1981) 450.
- [11] J. Kuti, J. Polónyi and K. Szlachányi, Phys. Lett. 98B (1981) 199.
- [12] B. Svetitsky and L. G. Yaffe, Nucl. Phys. B 210 [FS6] (1982) 423.
- [13] F. Karsch and E. Laermann, Phys. Rev. D 50 (1994) 6954.
- [14] J. Engels et al., Phys. Lett. 101B (1981) 89 and Nucl. Phys. B205 (1982) 545
- [15] F. Karsch, E. Laermann and A. Peikert, Phys. Lett. B 478 (2000) 447.
- [16] J. Engels et al., Z. Phys. C 42 (1989) 341.
- [17] E. Shuryak and I. Zahed, Phys. Rev. C 70 (2004) 021901.
- [18] J. Engels et al., Z. Phys. C 42 (1989) 341.
- [19] V. Goloviznin and H. Satz, Z. Phys. C 57 (1993) 671.
- [20] F. Karsch, A. Patkos and P. Petreczky, Phys. Lett. B 401 (1997) 69.

- [21] C. Aubin et al. (MILC Collaboration), Phys. Rev. D70 (2004) 094505;
A. Gray et al., Phys. Rev. D72 (2005) 0894507,
M. Cheng et al., arXiv:hep-lat/0608013
- [22] Z. Fodor and S. Katz, JHEP 0203 (2002) 014.
- [23] P. de Forcrand and O. Philipsen, Nucl. Phys. B 642 (2002) 290.
- [24] M.-P. Lombardo, Phys. Rev. D 67 (2003) 014505.
- [25] C. R. Allton et al., Phys. Rev. D 68 (2003) 014507.
- [26] G. Baym, Physics 96A (1979) 131;
T. Çelik, F. Karsch and H. Satz, Phys. Lett. 97B (1980) 128;
H. Satz, Nucl. Phys. A642 (1998) 130c.
- [27] D. Stauffer and A. Aharony, *Introduction to Percolation Theory*, Taylor and Francis, London 1994.
- [28] C. M. Fortuin, P. W. Kasteleyn J. Phys. Soc. Japan 26 (Suppl.), 11 (1969);
Physica 57, 536 (1972).
- [29] J. Cleymans and H. Satz, Z. Phys. C57 (1993) 135;
K. Redlich et al., Nucl. Phys. A 566 (1994) 391;
P. Braun-Munzinger et al., Phys. Lett. B344 (1995) 43;
F. Becattini, Z. Phys. C69 (1996) 485;
F. Becattini and U. Heinz, Z. Phys. C76 (1997) 268.
- [30] L. D. Landau, Izv. Akad. Nauk, Ser. Fiz. 17 (1953) 51;
J.-P. Blaizot and J.-Y. Ollitrault, in *Quark-Gluon Plasma 2*, R. C. Hwa (Ed.), World Scientific, Singapore 1990;
U. Heinz, P. F. Kolb and J. Sollfrank, Phys. Rev. C62 (2000) 054909.
- [31] E.V. Shuryak, Phys. Rep. 61 (1980) 71;
K. Kajantie and H.I. Miettinen, Z. Phys. C 9 (1981)
- [32] S. Datta et al., PR D69 (2004) 094507;
G. Aarts et al., Phys. Rev. D67 (2007) 0945413 and literature given there.
- [33] T. Matsui and H. Satz, Phys. Lett. B178 (1986) 416.
- [34] F. Karsch and H. Satz, Z. Phys. C 51 (1991) 209.
- [35] J.D. Bjorken, Fermilab-Pub-82/59-THY (1982) and Erratum;
M. Gyulassy and X.-N. Wang, Nucl. Phys. B420 (1994) 583;
R. Baier et al., Phys. Lett. B 345 (1995);
B. G. Zakharov, JETP Letters 63 (1996) 952.